Dynamic Mechanical Properties of Polypropylene–Polyamide Blends: Effect of Compatibilization

ZHIZHONG LIANG and H. LEVERNE WILLIAMS*

Department of Chemical Engineering and Applied Chemistry, University of Toronto, Toronto, Ontario, Canada M5S 1A4

SYNOPSIS

The influence of compatibilization on the dynamic mechanical properties of polypropylene (PP) binary blends with polyamide-11 (PA) has been investigated. In the blends an acrylic acid functionized PP was used as a blend component and compared with nonfunctionized PP over the whole concentration range. The results demonstrate that the use of the functionized PP instead of the unmodified one produced blends with different dynamic mechanical properties due to adhesion enhancement between the two phases. The storage moduli E' of the compatibilized blends vary nearly linearly as a function of composition over a broad temperature region, whereas those of the noncompatibilized ones deviate greatly from linearity, specially at about 50/50 ratio, at which a minimum exists at about room temperature. While the dynamic testing gives no evidence for the variation in the glassy transition temperatures (peak maxima) of the components (PP and PA) in the two types of blends, both the loss modulus (E'') and the loss factor (tan δ) data indicate that the compatibilized blends differ from the noncompatibilized ones mainly in the glassy transition (β relaxation) process of the PA phase, suggesting that the compatibilization of the blends seems to influence the PA phase more than the PP phase included. But, for the β-relaxation behavior of the PA in the modified blends, the tan δ spectrum shows a more complex pattern than does the E''. These results are discussed in terms of the morphological texture of the blends and possible chemical or physical interactions between the two constituent polymers.

INTRODUCTION

Immiscible polymer blends are often preferred over the miscible types since they may combine the most desirable properties of both polymer components, while avoiding their major drawbacks. The key to obtaining satisfactory performance in immiscible blends is to minimize interfacial tension and to improve adhesion between the two phases, resulting in a more finely dispersed phase, greater resistance to gross separation, and improved overall properties.[1,2] The blends are, then, to be considered effectively compatibilized.[3,4]

It is known that such compatibilization of immiscible blends can be achieved mainly by introducing a graft or block copolymer with segments capable of specific interactions, and/or chemical reactions with the blend components. This copolymer additive, generally referred to as a compatibilizer, can either be added as a third component in the blend or can be formed in situ during melt blending. In the latter case a functionized polymer with organic group(s) reactive toward one of the components and soluble in the other should be chosen.[5,6]

Polypropylene (PP), among polyolefins (PO), is a most important polymer for its intrinsic properties such as a high melting temperature, low density, high chemical inertness, and the capability of being produced with different morphological and molecular structures, of being reinforced with high amounts of fillers, and of being toughened with elastomers.[7] In addition, PP can be modified by grafting on functional groups to make it possible that PP can be blended with some polar polymers [such as polyamide (PA), poly(ethylene terephthalate),[3,8] and polycarbonate[9]] for exploring its ability to fur-

* To whom correspondence should be addressed.

Journal of Applied Polymer Science, Vol. 44, 699–717 (1992)
 CCC 0021-8995/92/040699-19$04.00

ther compete with technopolymers in some important, rapidly growing application sectors.

For PP–PA blends, Ide and Hasegawa[10] added maleic anhydride (MA) functionized PP graft copolymer (PP-*g*-MA) to the binary blend and obtained almost homogeneous morphology. Similar compatibilizations by adding functionized PP copolymers with MA or carboxylic acid (COOH) groups were also reported for PO–PA blends by other authors.[10–16] Chuang and Han[11] measured the rheological properties of blends of PA with an ethylene-based multifunctional polymer and suggested the possibility of chemical interaction between the PA and PO phases. Macknight and his co-workers[6] confirmed the possibility of an amidation reaction between the NH_2 terminal groups of the PA and the COOH groups of the copolymer in a study on the chemical modification in polyethylene (PE)/PA-6 blends. Fairley and Prud'homme[12] discussed the possible interactions between the components in the amorphous and in the crystalline phases based on the results on the binary PE/poly(ethylene-co-methacrylic acid) (EMA) and PA-6/EMA blends mainly by differential scanning calorimetry and stress–strain measurements. Willis and Favis[13] determined the emulsifying effect of an ionomer [poly(ethylene–methylacrylic acid–isobutylacrylate terpolymer)] on the morphology of the ternary PO–PA blends. However, there has been little done with detailed studies on dynamic mechanical properties of the compatibilized PP–PA blends, although dynamic mechanical investigations are extensively used for elucidation of the phase structure of the blends.

The objective of this work is to investigate the effect of compatibilization through chemical modification during melt mixing on the dynamic mechanical properties of the blends of PP-based resins with polyamide-11 (PA-11) over the whole composition range. We used functionized PP (PP-*g*-acrylic acid) as a blend component and compared the modified blends with unmodified PP blends with PA-11. The choice of PA-11 among the PA was prompted by two considerations: the highest moisture resistance and the processing temperature closest to that of PP.

EXPERIMENTAL

Materials

Polyamide 11 (PA-11) in pellet form (34667) was supplied by Rilsan Industrial Inc. Polypropylene was Profax 6631 (MFI = 2, Himont Canada Inc.) and the acrylic acid grafted polypropylene copolymer (PP-*g*-AA) was Polybond 1001 in pellet form (6% acrylic acid, MFI = 40, BP Performance Plastics).

Blend Preparation

For blending, commercial grades of the polymers were used as received. Blends were prepared by first mixing the well-dried pellets thoroughly, followed by melt mixing in a co-rotating twin-screw extruder (C. W. Brabender) equipped with a rod die and operating at 210–240°C. The blended samples were subsequently quenched in water, then ground in a C. W. Brabender granulator (Model S 20/9) into chips and dried *in vacuo* for 3 days at 80°C. The dried chips were used to measure melt viscosity and to make compression molded sheets for dynamic mechanical observation. All the pure polymers were also subjected to the same procedures in order to compare the behaviors of the blends studied with those of the components.

Melt Viscosity Measurement

The rheological data of the pure polymers and the blends were obtained using a Brabender Plasticorder (type 230V8) equipped with a mixer of 60 cm^3 volume. The right charge weight for the mixer for all the blends was defined according to the density of the blends of varying blend ratio. The density of the blends was calculated from the additive formulas of mixture. The test was run for 8 min. The temperature inside the mixing chamber was 220°C and the speed of the rollers was 100 rpm.

Specimen Preparation

From the blends prepared earlier, sheets of 2.95 mm thickness were obtained by compression molding in a heated press equipped with a water cooling system. The samples were heated to 210°C and kept 4 min between the plates without any applied pressure, allowing for complete melting. After this period, a press of 20 tons was applied at the same temperature for 5 min. The samples then slowly cooled in another unheated press to room temperature for about 10 min. From the sheets so prepared, the rectangular specimens were cut to perform the dynamic mechanical tests.

Dynamic Mechanical Measurements

Measurement of dynamic mechanical properties (the dynamic storage and loss moduli E' and E'' and

the loss factor tan δ) as a function of temperature were made by using an Imass automated dynamic mechanical analyzer (Dynastat). In order to obtain the PA-11 samples containing different relative humidity and to observe the effect of humidity on the dynamic mechanical analysis (DMA) data of the PA-11 specimens, the PA specimens (PA-11 and its blends) were selectively treated before testing through the following different drying conditions: (a) C_1 was the sample placed in a moist environment at room temperature for 3 weeks, (b) C_2, C_3, and C_4 were samples dried in a vacuum oven at 80°C for 6, 16, and 96 h, respectively.

The testing was carried out in three-point bending (flexure) and in the low-range displacement control mode. The static and the dynamic loads were 2 and 1 kg, respectively. The frequency was usually 1 Hz. The temperature ranges were from −145, −100, or −30 to +110°C, depending on the polymers or the blends tested. The magnitude of the dynamic tensile moduli (E' and E'') and the tangent of the phase angle (tan $\delta = E''/E'$) were measured at about every 5°C with increasing temperature.

Morphological Observations

A scanning electron microscope (SEM: Hitachi S-520) was used to observe the morphology of the blends. The samples for SEM were obtained from the cryogenically fractured surface of the DMA specimens, obtained by cutting from the compression-molded sheets. The fractured surface was coated with gold using an Edwards E 306A SEM coating unit.

RESULTS AND DISCUSSION

PP Components

Nonfunctionized PP (Profax 6631) and functionized PP (Polybond 1001 G) are presented in Figures 1 and 2 with their temperature dependence of the dynamic storage and loss moduli (E' and E'') and the loss factor (tan δ) at 1 Hz. In the temperature range between −100 and +110°C, polypropylene may show three dynamic mechanical relaxations. The dominant relaxation on the DMA spectra for PP is the β relaxation at about 0°C (on the E'' curves) or 5°C (on the tan δ curves), which is generally recognized to be the glass-rubber relaxation of amorphous portions of the PP solid, while the less intensive and broader peaks on the tan δ and the E'' curves at around the −80°C may be associated with the γ relaxation, which is attributed to the relaxing unit consisting of a few chain segments rather than in-

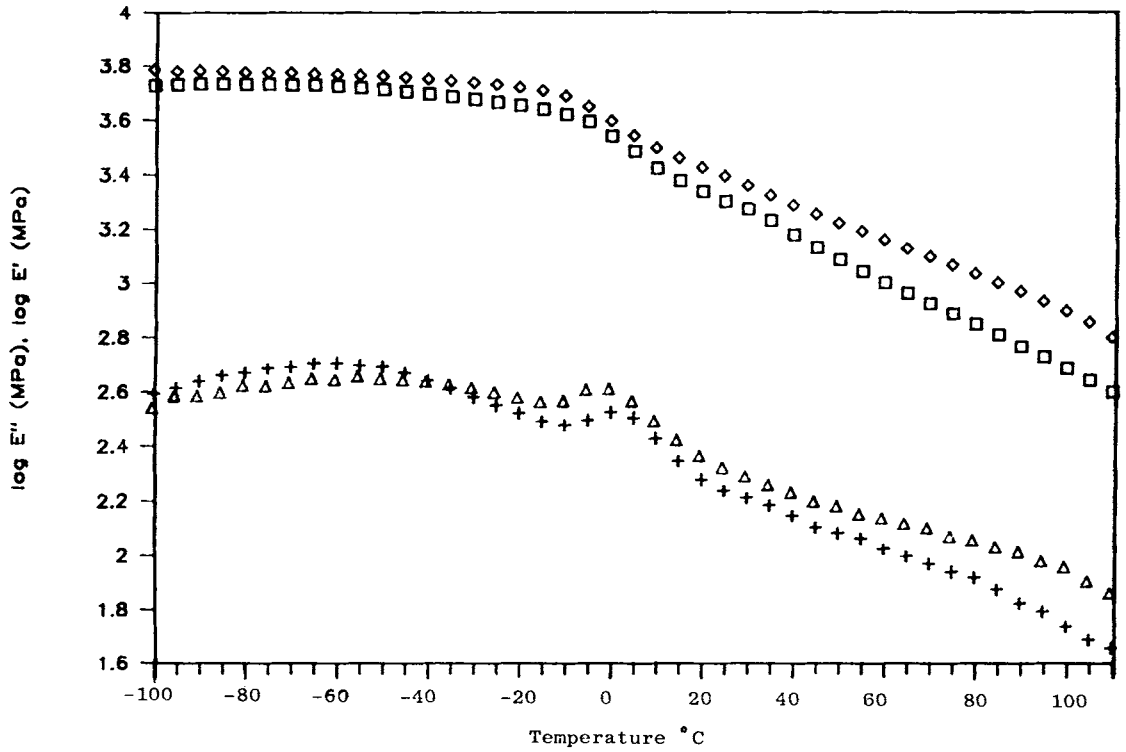

Figure 1 Temperature dependence of storage modulus E' and loss modulus E'' at 1 Hz for Profax 6631 (□, +) and Polybond 1001 (◇, △).

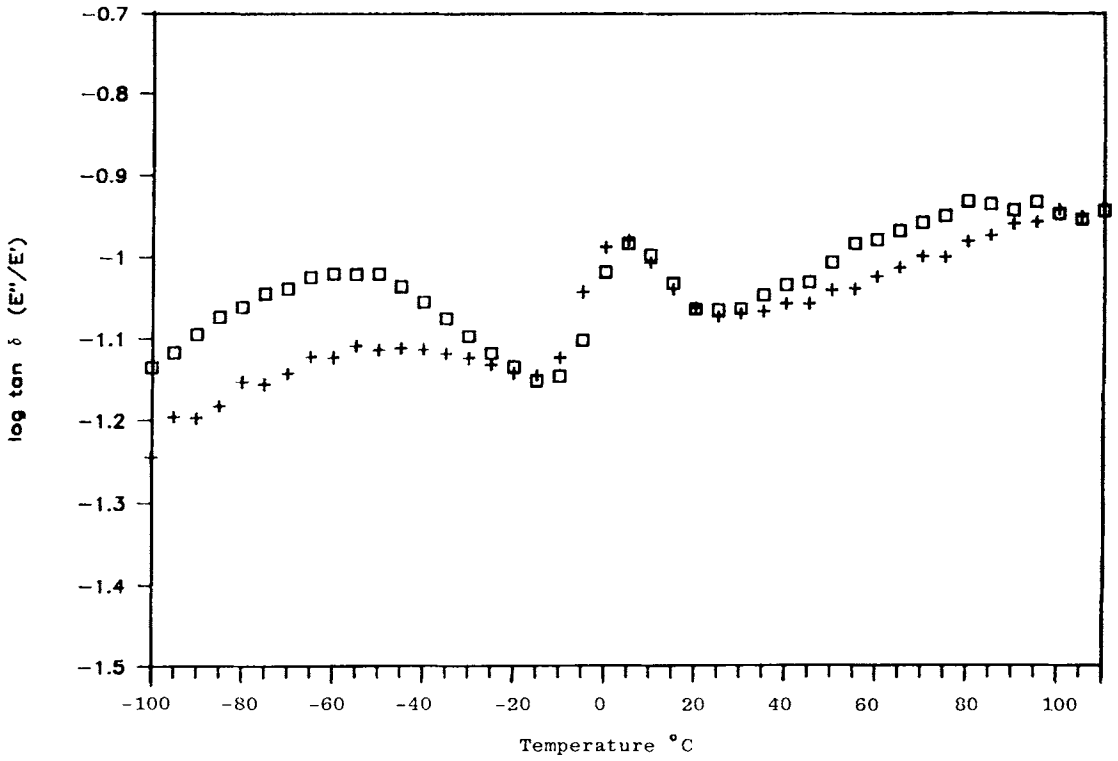

Figure 2 Temperature dependence of loss factor tan δ at 1 Hz for Profax 6631 (□) and Polybond 1001 (+).

volving the motion of more complex morphological units of PP.[17] The weak peak, which appeared as a shoulder at about 70–100°C, is associated with the crystalline regions of PP, and the properties of this relaxation strongly depend on the crystal morphology.[18] The data measured for the transitions of PP resins are basically consistent with the data reported in the literature.[19]

It can be seen from Figures 1 and 2 that the two different PP polymers used have distinguishable features in their relaxation behaviors. The functionized PP (Polybond 1001) shows higher stiffness than the nonfunctionized PP (Profax 6631), while Polybond 1001 has the same glassy transition process as Profax 6631. In addition, the γ relaxation of Profax 6631 is obviously more intense than that of Polybond 1001, and the shoulder on the low-temperature side of the transition associated with the PP crystalline region is shifted to a lower temperature. The reason for this may be due to the existence of the ethylene–propylene copolymer (EPM) units in Profax 6631, which is a commercial PP block copolymer. EPM as a minor component in the PP molecules could have its own β-glassy relaxation process at around −50 to −60°C,[20] and its existence may increase the intensity and breadth of the γ-transition peak of PP. Moreover, the EPM phase inclusion in PP could cause a damaged, irregular spherulitic structure.[21] This may be a reason for the crystalline-related relaxation to commence at a lower temperature, since this transition peak of PP is strongly dependent on the PP crystal morphology.[18]

PA Component

In Figure 3 the temperature dependence of the dynamic storage and loss moduli (E' and E'') and the loss factor (tan δ) at 1 Hz for PA-11 are given. Both the tan δ and the E'' curves show that there are three well-defined mechanical relaxations in a temperature range between −145 and +110°C. The three loss peaks on the tan δ curve occur at about −120, −60, and +60°C, respectively. These values are consistent with the data reported by other authors[19] for PA-11. The largest peak (or β transition) at about 60°C is attributed to the movement of large-chain segments set free by the disappearance of hydrogen bonding with increasing temperature, while the peak at about −60°C (or $T < T_\beta$ peak) may be explained by a crankshaft-type motion involving an unbonded amide group and several methylene carbon groups.[22]

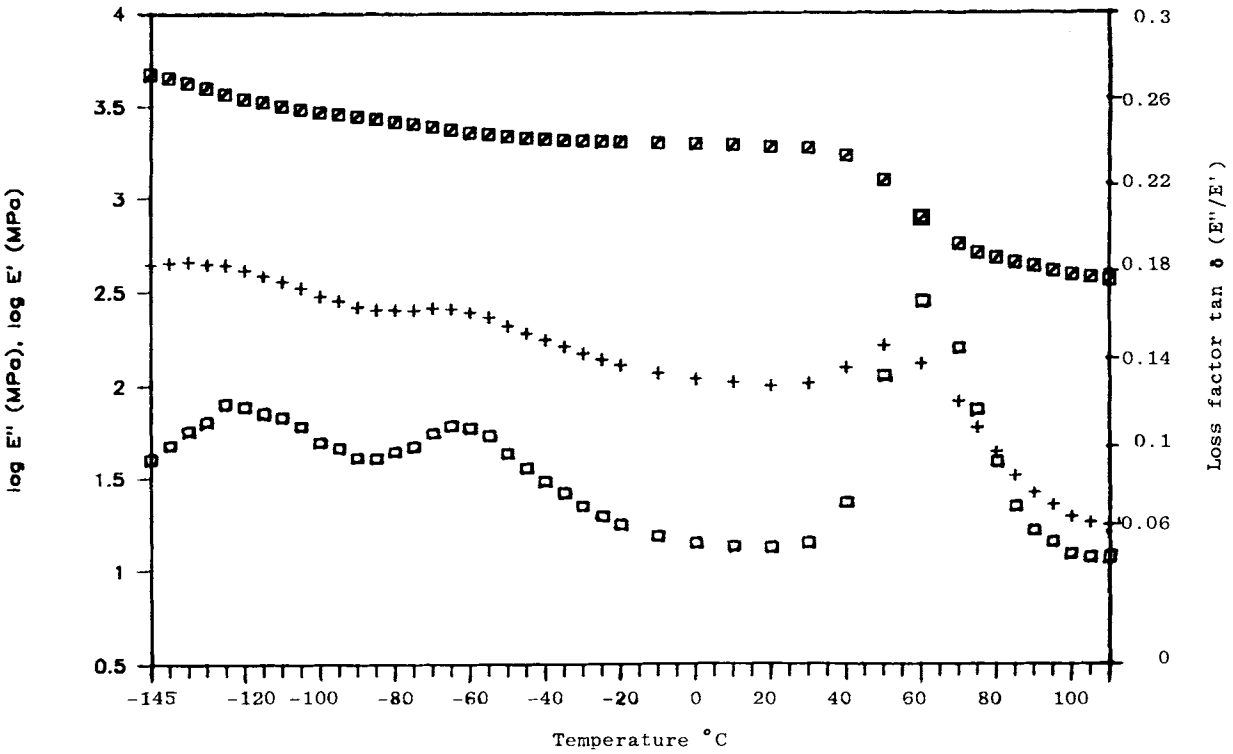

Figure 3 Temperature dependence of E' (⊠), E'' (+), and tan δ (□) at 1 Hz for PA-11 (treated under C_2 conditioning).

The $T < T_\beta$ peak is strongly dependent on the moisture content in polyamides. The γ transition at about −120°C is a consequence of cooperative motion of the methylene groups between amide linkages.[23]

Although the β transition (T_β) is considered by many authors to be the glassy transition (T_g) of the polyamide, there have been doubts about the nature of this relaxation mainly due to two uncertainties: (1) the low sensitivity of its location in the temperature scale to variation in the length of the aliphatic chain and (2) the position of the crystalline α–γ transition, which appears to be superimposed on the β (amorphous) relaxation.[24,25] However, this article is not intended to comment upon questions regarding the definition of the β transition.

Figures 4, 5, and 6 summarize the results regarding the effect of the moisture on the dynamic mechanical properties of PA-11. Although it has been recognized for years that the absorbed moisture in polyamide can greatly affect the position of the β relaxation and the strength of the $T < T_\beta$ damping peak of polyamide (specially for PA-6), the experimental observation in this study was aimed at defining reasonable drying and testing conditions for PA-11, which would be used to be blended with PP to get reliable analysis data of dynamic mechanical properties.

The results from Figures 4 and 5 indicate that the absorbed water in C_1 PA specimens (placed under a moisture environment at about 20°C for 3 weeks) caused a shift of the β-transition peak to a lower temperature and greatly increased the $T < T_\beta$ peak in intensity at the same time. Low moisture content in the other PA samples (C_2 and C_3) significantly influenced the magnitude of the $T < T_\beta$ peak, while the β-transition peak showed very low sensitivity to the moisture at low content in the PA-11. For the "dried" PA-11 sample (under C_4 condition), the $T < T_\beta$ peak decreased further in height and was almost eliminated by "drying" (see C_4 curves in Figs. 4 and 5). In Figure 6 the effect of moisture on the storage modulus (E') of PA-11 over a broad temperature range is represented. In the high-temperature region around the β-transition zone, E' data for the C_1 PA sample with a high moisture content shows a distinct transition that was shifted to a lower temperature, and other samples (C_2, C_3, and C_4) with varying moisture at lower levels have the same relaxation behavior basically. In the low-temperature region the E' of PA-11 shows a steep decrease as the temperature approaches the T

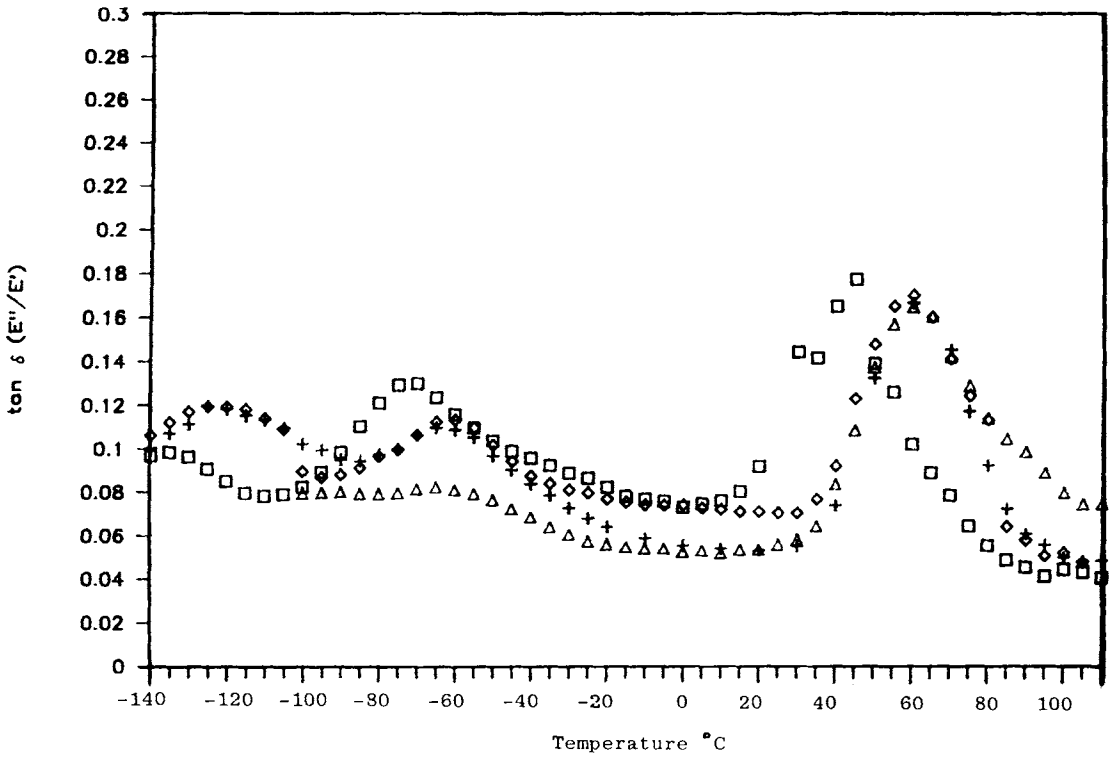

Figure 4 Temperature dependence of tan δ at 1 Hz for PA-11 treated under various conditioning (C_1: □, C_2: +, C_3: ◇, and C_4: △).

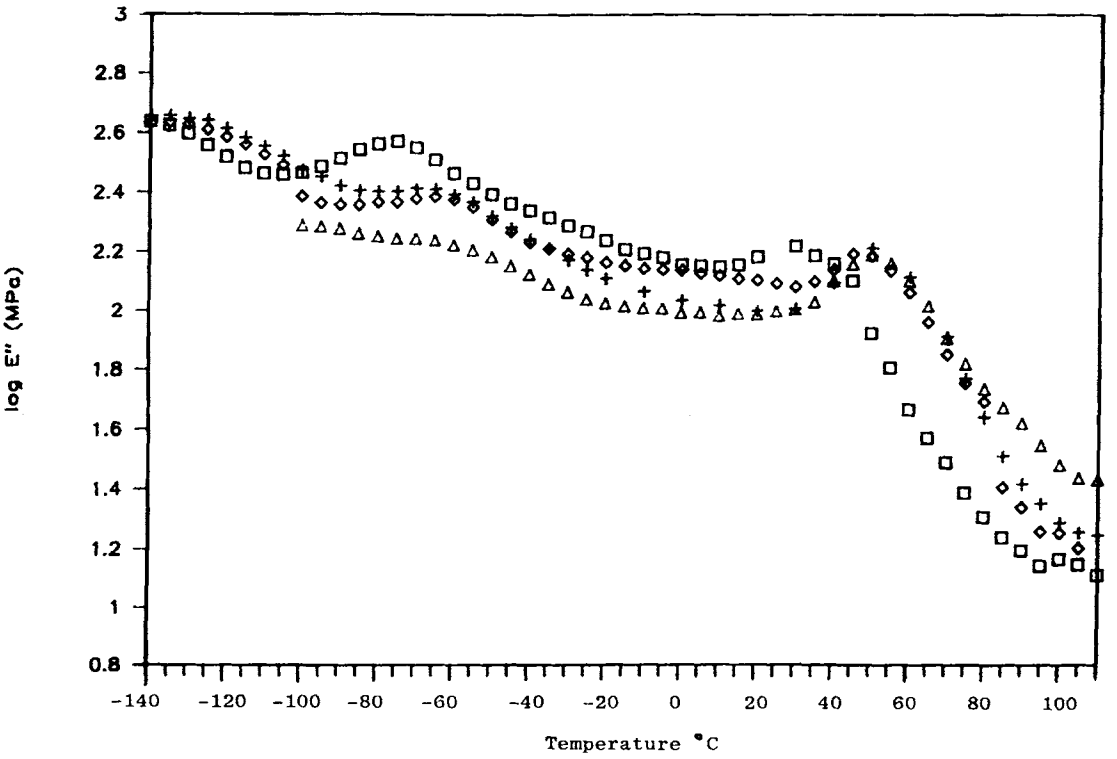

Figure 5 Temperature dependence of E'' at 1 Hz for PA-11 treated under various conditioning (C_1: □, C_2: +, C_3: ◇, and C_4: △).

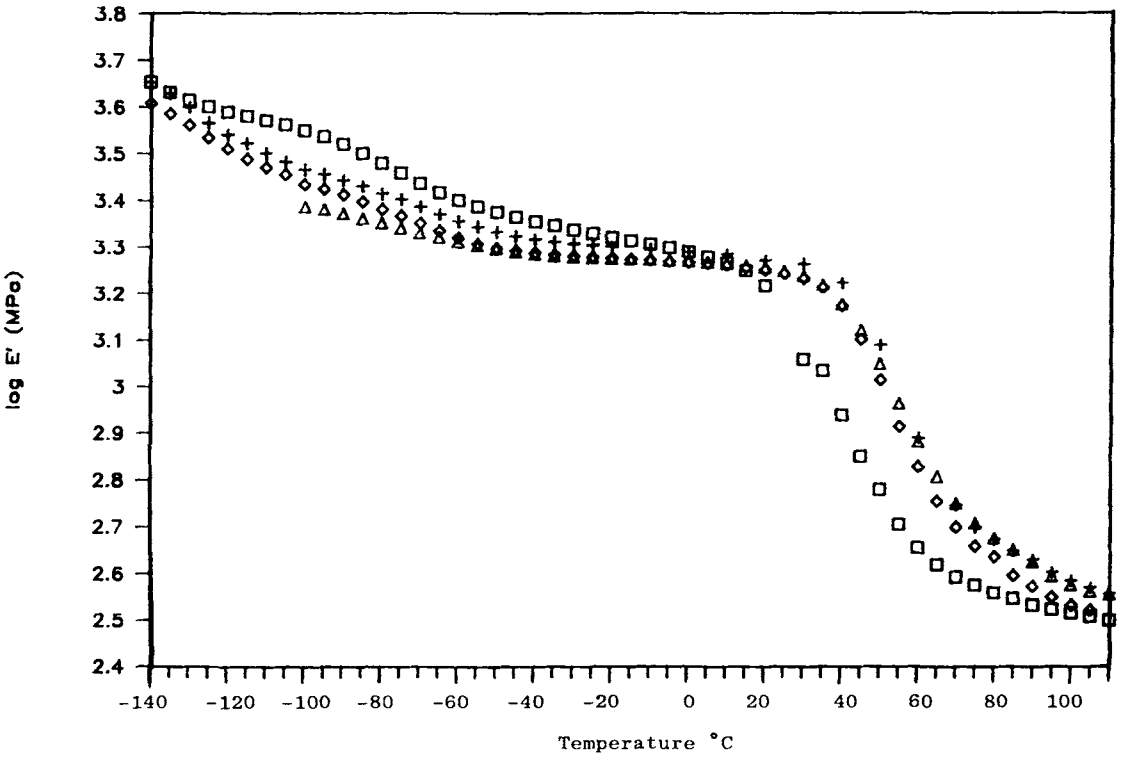

Figure 6 Temperature dependence of E' at 1 Hz for PA-11 treated under various conditioning (C_1: □, C_2: +, C_3: ◇, and C_4: △).

$< T_\beta$ transition, followed by a plateau zone until the onset of the β-transition process. The more moisture the PA-11 specimens contain, the more their E' results increase.

It is thus clear that the results in this section indicate the significance of observing the effect of drying conditioning on the dynamic mechanical properties of the PA-11 component in the study of the PP–PA blends. The specimens through C_4 conditioning will be considered to be "dry" in the study, and all blends involved were treated before testing according to the C_4 conditioning.

Noncompatibilized PP–PA Blends

The dynamic mechanical data for the noncompatibilized PP–PA-11 blends over the whole range of composition, viz., the storage and loss moduli (E' and E'') and the loss factor (tan δ) as a function of temperature, are shown in Figures 7–11.

The loss factor curves (tan δ) shown in Figure 7 for the noncompatibilized blends exhibit two fairly sharp relaxation peaks at 5 and 60°C, each exactly corresponding to the glassy transition temperatures of PP and PA, respectively. However, the other secondary relaxation processes on the tan δ curves could be interpreted with difficulty, due to the overlapping of the multiple motion units involved in the PP phase and the PA phase in the same temperature range. Usually, the dynamic mechanical data from the loss modulus (E') curve could reflect more real relaxation behavior of polymer materials. The main relaxation processes in the amorphous region for the PP phase and the PA in the blends can also be detected in the loss modulus curve (shown in Fig. 8). But the loss peaks are much less intense than the corresponding ones on the tan δ curves, specially for the β-transition peak for the PA phase in the blends. Figure 9 gives a local magnification of the relaxation processes discussed. It is thus clear that the two main mechanical relaxation behaviors of the noncompatibilized blends do only represent a simple addition of the β transition of PP and the β transition of PA, indicating weak mechanical interactions between two phase (PP and PA) in the blends.

The typical incompatibility of the blends could be more obviously reflected from the in-phase modulus (E') behavior (shown in Fig. 10) of the noncompatibilized blends at various PP–PA ratio. It is interesting to note that in a broad low-temperature range from −100 to 20°C, the modulus of the PP (or PA) enriched blends showed low dependence on

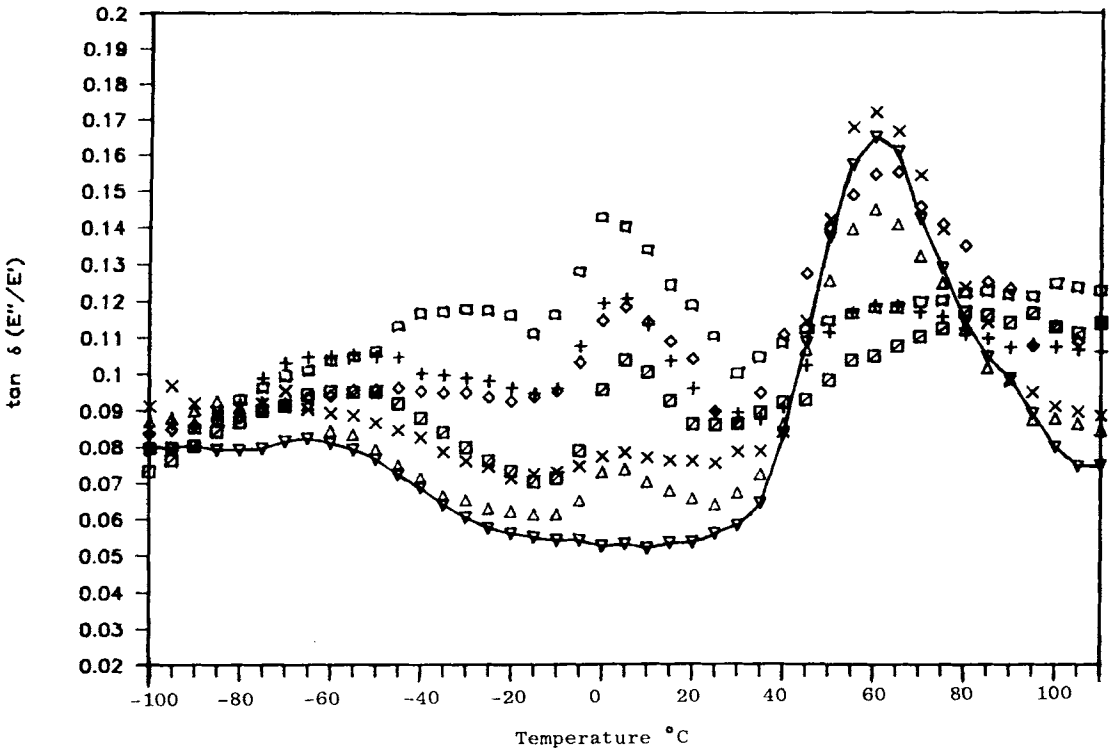

Figure 7 Variation in tan δ with temperature for noncompatibilized blends at various (PP–PA) ratios (10/0: ⊠, 9/1: □, 7/3: +, 5/5: ◇, 3/7: △, 1/9: ×, 0/10: ▽).

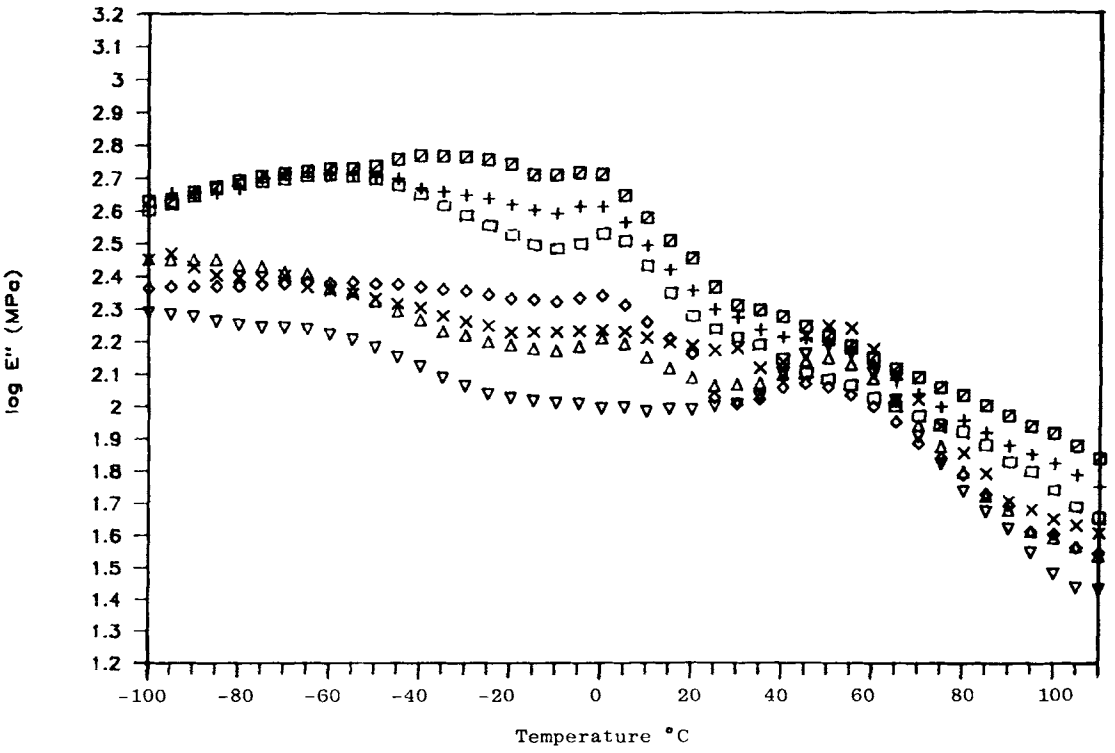

Figure 8 Variation in E'' with temperature for noncompatibilized blends at various (PP–PA) ratios (10/0: □, 9/1: ⊠, 7/3: +, 5/5: ◇, 3/7: △, 1/9: ×, 0/10: ▽).

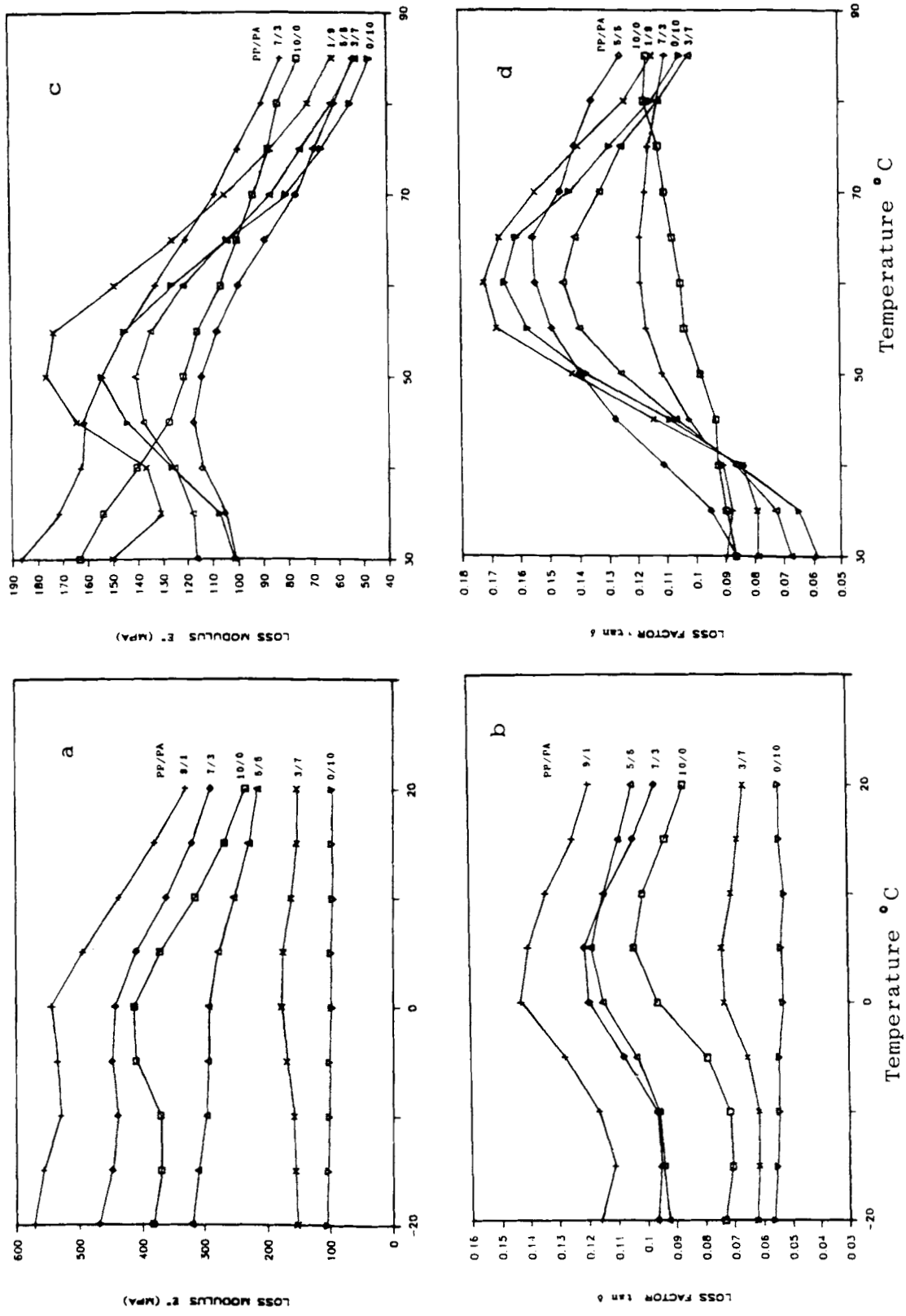

Figure 9 β relaxation for PP phase (a, b) and β-relaxation for PA phase (c, d) in the noncompatibilized blends at various ratios.

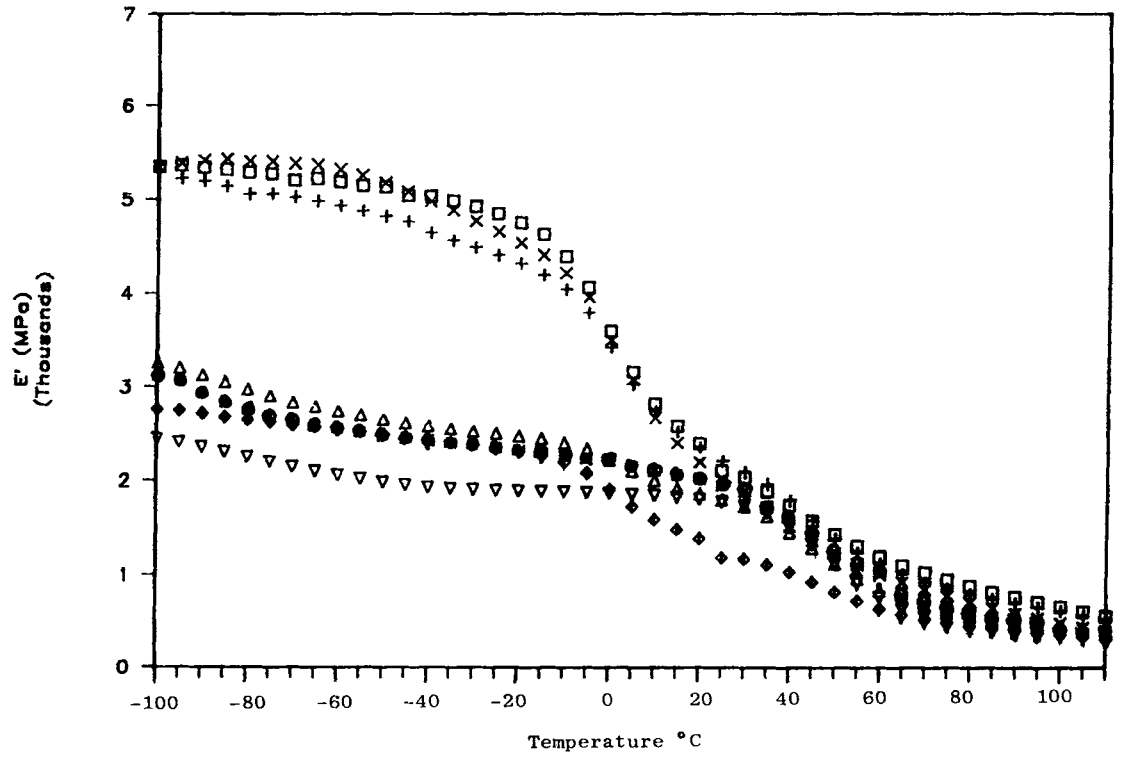

Figure 10 Variation in E' with temperature for noncompatibilized blends at various (PP–PA) ratios (10/0: ×, 9/1: □, 7/3: +, 5/5: ◊, 3/7: △, 1/9: ⊗, 0/10: ▽).

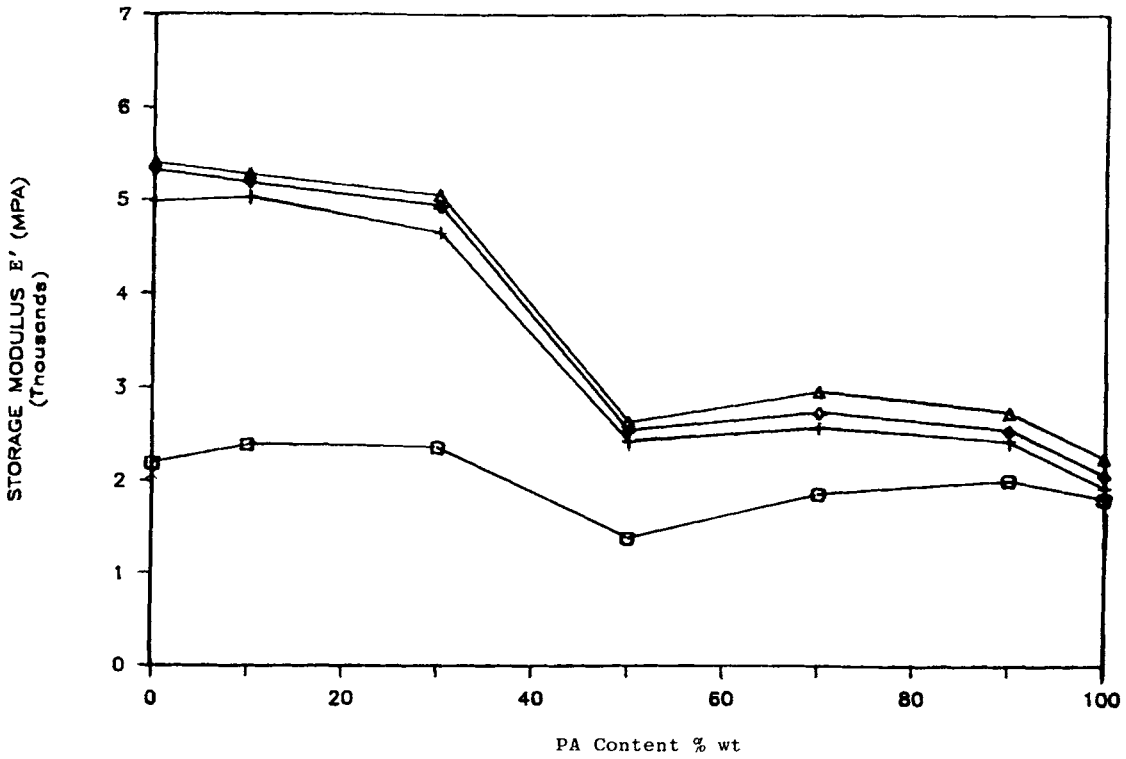

Figure 11 Storage moduli E' of noncompatibilized blends as a function of PA content at various temperatures (20°C: □, −40°C: +, −60°C: ◇, −80°C: △).

the content of the second blend component. The E' curves for the blends approach those for the matrix materials, especially for the PP-enriched blends. However, the PP–PA blend at 50/50 ratio shows an abnormal decrease in modulus. In Figure 11 the moduli of the blends are plotted as a function of PA content at various temperatures. The variation in moduli of the binary blends with the blend composition exhibits obviously negative deviation from linearity when the concentration of the two components is comparable. At about room temperature the modulus of the blends at this composition is even lower than those of either component.

This behavior could be explained from SEM micrographs (Fig. 12) obtained for the corresponding blend specimens. If the content of PA (or PP) is less than about 30 wt %, the blend is composed of a PP (or PA) matrix in which well-shaped spherical PA (or PP) particles are embedded [see Fig. 12 (a), (b), (d), and (e)]. In this figure the domain surface and the surface of the hole left by a large number of domains pulled away from their previous position during the fracture process appear to be very smooth, strongly suggesting a poor interfacial adhesion in the noncompatibilized PP–PA blends. Therefore, the dispersed phase is of a larger size and has relatively smaller contact areas with the matrix in contrast to a finer dispersion. Under this circumstance some properties such as modulus or stiffness of the blends depend mainly on the properties of the matrix. With increasing volume fraction of the dispersion phase, the properties of blends should be more

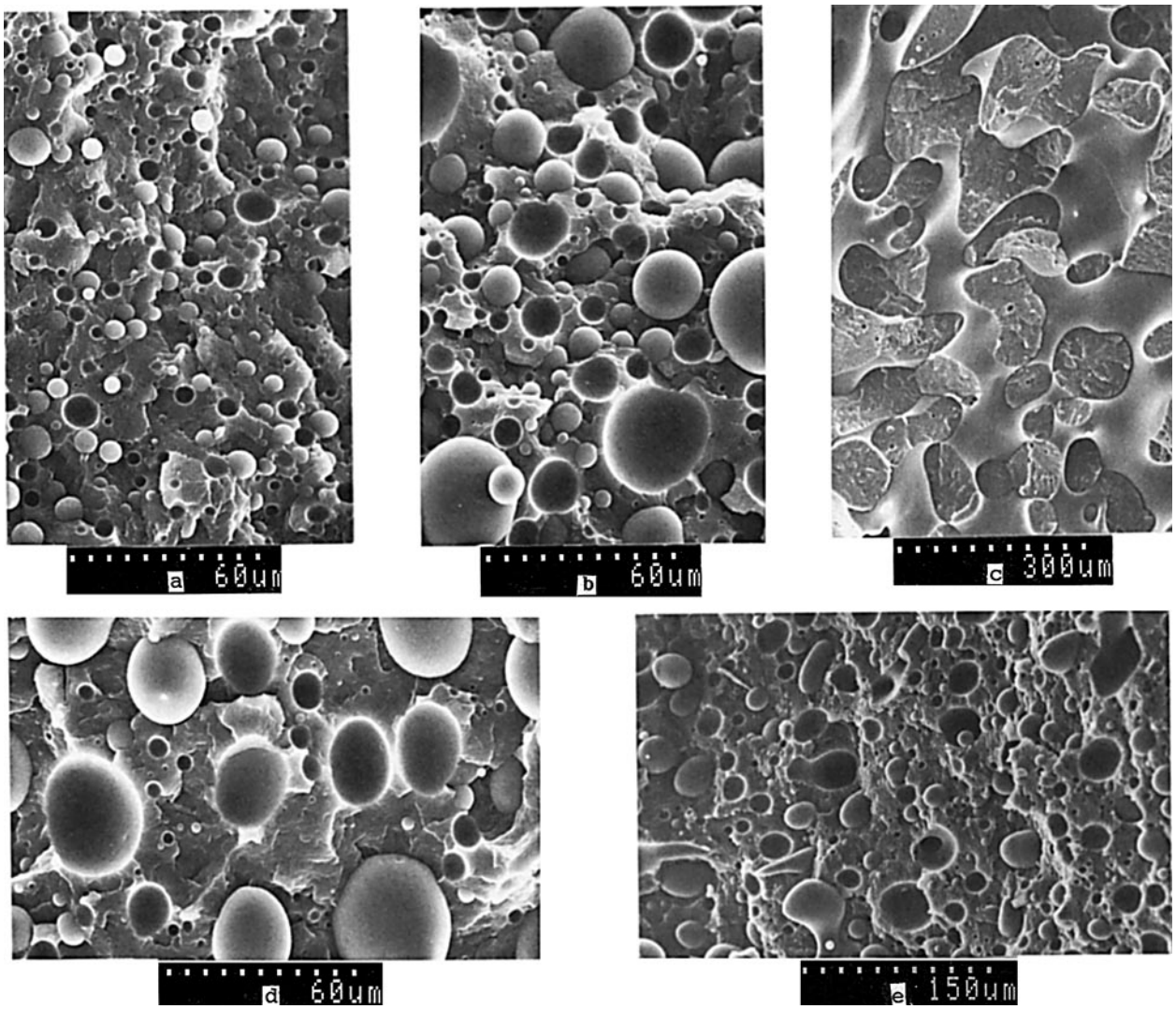

Figure 12 Scanning electron micrograph of fractured surfaces for the noncompatibilized blends with various PP/PA ratios (a) 1/9, (b) 3/7, (c) 5/5, (d) 7/3, (e) 9/1.

influenced, however, the extent of being influenced is related to those factors such as the size and shape of the dispersed phase as well as the interfacial tension and contact areas between the particles and matrix.[26]

The PP–PA specimen at 50/50 blend ratio shows a co-continuous two-phase interpenetrating morphology [see Fig. 12(c)]. This composition may attain a maximal contact area[27] and leads to the poorest balance of properties due to very weak mechanical interactions between the two phases.[28] The storage modulus of the blends can decrease greatly, due to this very poor interphase adhesion, to the much lower values than those predicted on the basis of an additive rule. In addition, at about 20°C, full motion of multiple structure units involved in the PP and the PA could also provide more free volume for the noncompatibilized blends, which may also be a factor to reduce the E' value of the materials. Actually, the appearance of the noncompatibilized blend sheets at 50/50 ratio more or less looks like a PP foam with a void content, which is much different from that of the compatibilized ones prepared under the same compression molding condition.

Some differences in morphologies between the PP-enriched blend with 10% PA and the PA-enriched blend with 10% PP can also be clearly visible in Figure 12. The PP particles in the PA-11 matrix have a smaller dimension, which ranges between about 1 and 10 μm, than the PA as a dispersed phase in the PP matrix, which ranges between 4 and 30 μm. This result is quite similar to the results obtained by other authors[29] on the noncompatibilized PE–PA blends, suggesting that some of the interaction exists in the interphase between the PE particles and the PA matrix at the high content of PA in the blends. The more finely dispersed particles at the same composition should have a larger influence on the properties of the matrix materials. This can be confirmed by the E' data obtained in this section.

Compatibilized PP–PA Blends

Figures 13–16 and 19 summarize the dynamic mechanical data for the compatibilized PP–PA blends over the whole composition. The results of this set of experiments show that the use of the functionized PP (Polybond 1001) instead of a nonfunctionized one does produce blends with different dynamic mechanical properties due to an improvement in com-

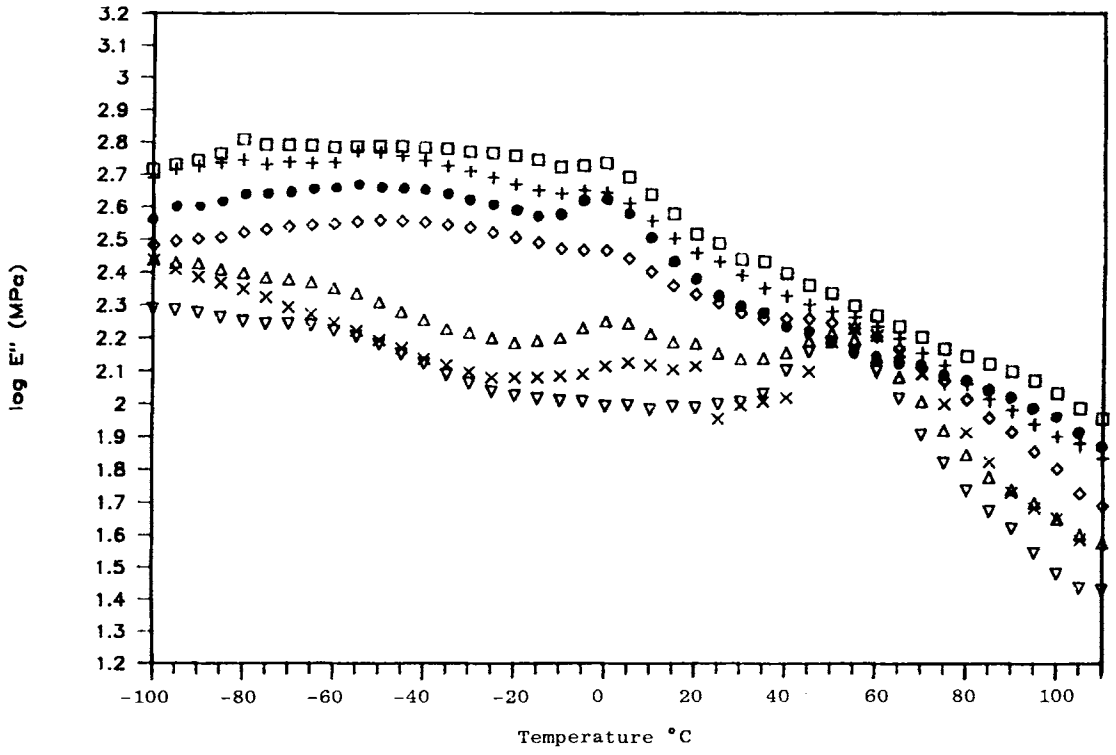

Figure 13 Variation in E'' with temperature for compatibilized blends at various (PP–PA) ratios (10/0: ●, 9/1: □, 7/3: +, 5/5: ◇, 3/7: △, 1/9: ×, 0/10: ▽).

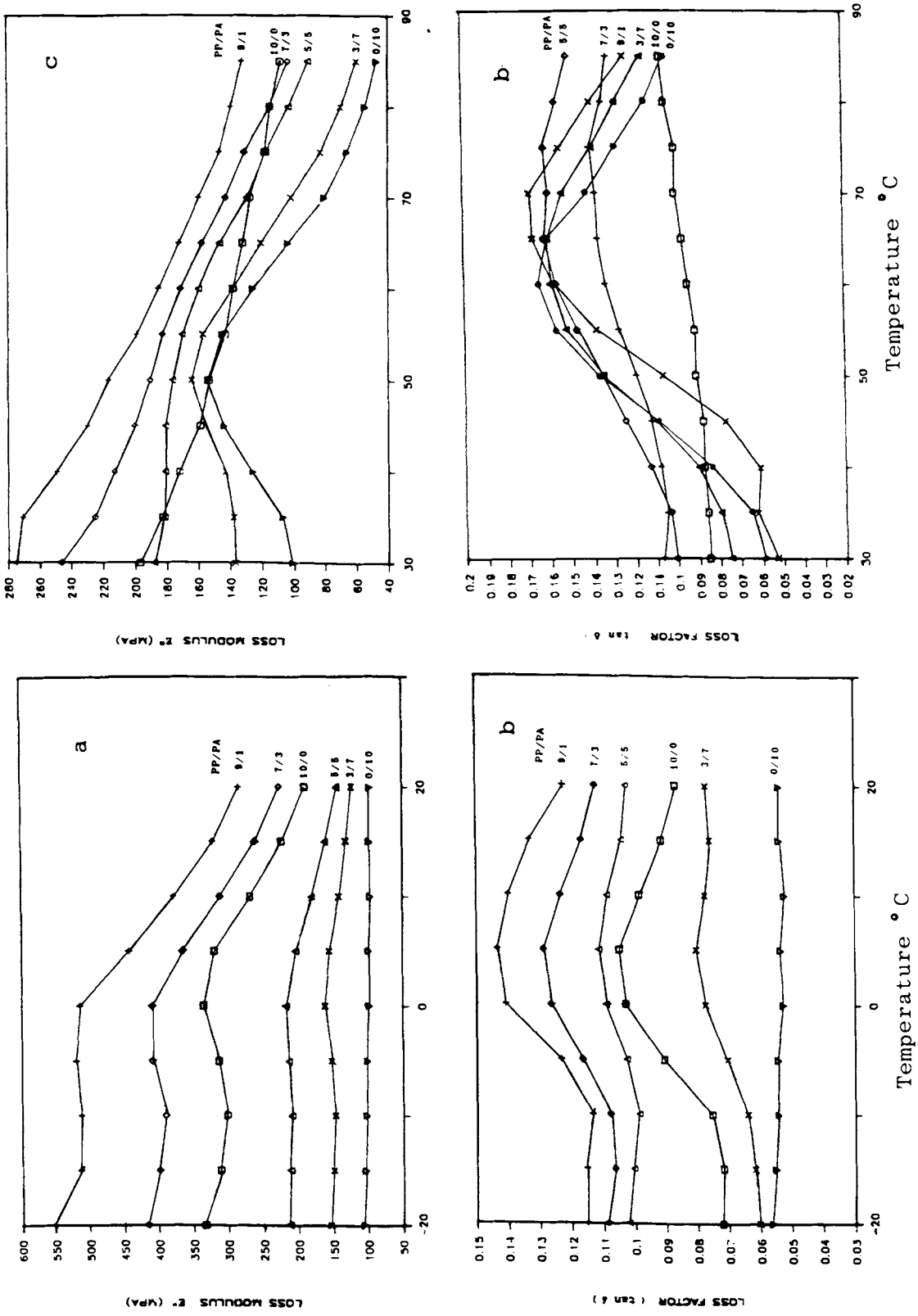

Figure 14 β relaxation for PP phase (a, b) and β-relaxation for PA phase (c, d) in the compatibilized blends at various ratios.

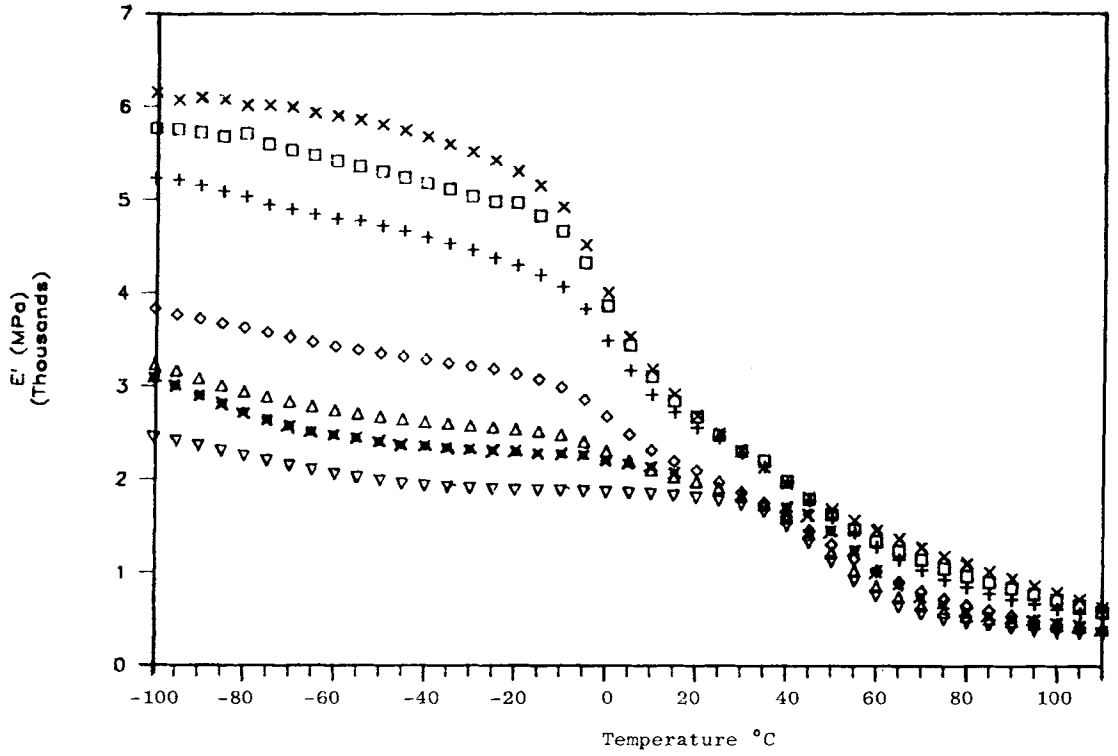

Figure 15 Variation in E' with temperature for compatibilized blends at various (PP–PA) ratios (10/0: ×, 9/1: □, 7/3: +, 5/5: ◇, 3/7: △, 1/9: ■, 0/10: ▽).

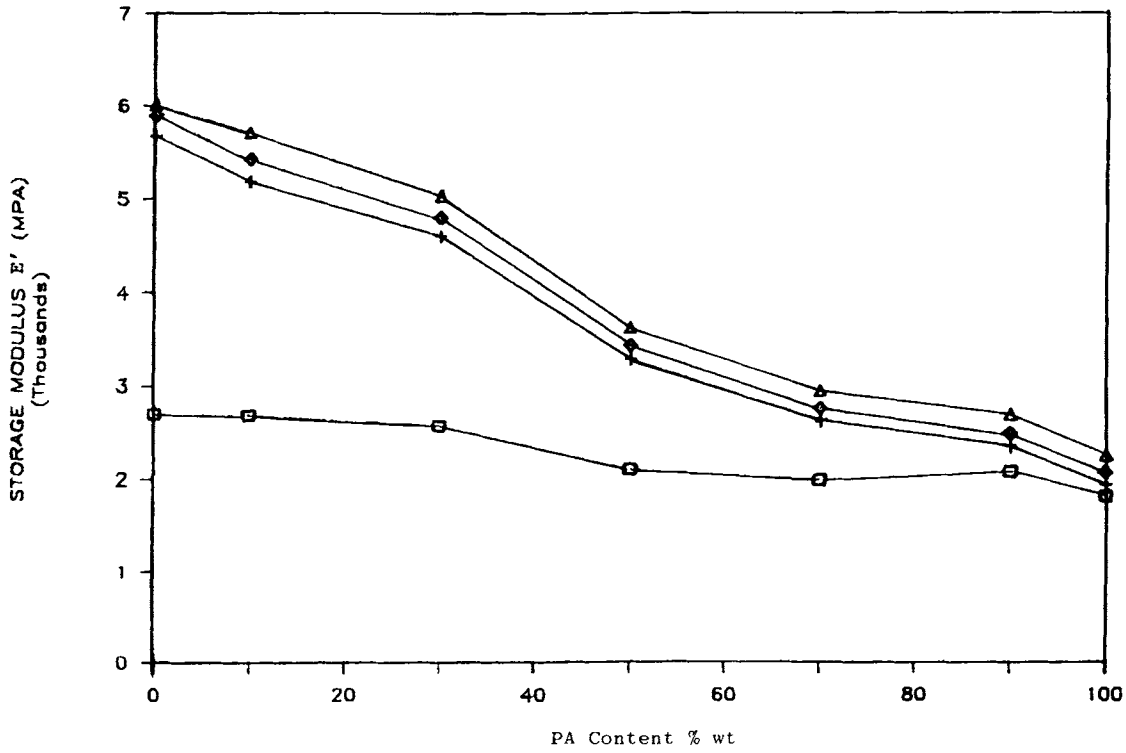

Figure 16 Storage moduli E' of compatibilized blends as a function of PA content at various temperatures (20°C: □, −40°C: +, −60°C: ◇, −80°C: △).

patibility between the PP phase and the PA phase in the blends.

The loss modulus E'' data from Figure 13 indicates that the compatibilized blends differ from the noncompatibilized blends in the β-relaxation (or glassy transition) process of the PA phase in the blends, while the glassy transition (T_g) of the PP phase in the two types of blends does not have an appreciable disparity. And the glassy transition temperatures (peak maxima) of the PA phase in the blends are not changed (or shifted) basically with the compatibilization in the whole composition. This testing result is similar to the E'' data presented, most recently, by Utracki and Sammut[30] for Orgalloy R-6000 [a commercial alloy of compatibilized PP–PA-6 (40/60) blend] in a study on flow of immiscible blends, suggesting that the compatibilization may affect the PA matrix more than the dispersed PP.

Further, closely checking up on the difference in the β peaks of the PA phases between the two types of blends, it can be found that the β-damping peaks for the PA in the compatibilized blends become broader at some compositions (shown in Fig. 14). At about 50/50 ratio, the blend exhibits only a shoulder-type peak on the low-temperature side of the β-transition zone of the PA phase, while the noncompatibilized blend at the same composition still maintains a well-shaped β peak of the PA (shown in Fig. 9). Although such a result can be readily interpreted in terms of partial miscibility, the E'' data in the section clearly suggest that the compatibilized PP–PA blends are not molecularly compatible and still have a two-phase morphological feature.

The storage modulus (E') data (shown in Fig. 15) seems to show more evidence for the partial miscibility in the compatibilized blending system studied. In comparison with the noncompatibilized ones (as in Fig. 10), the functionized PP blends with PA-11 reveal much more E' composition dependence in a broad temperature range tested from -100 to $+20$°C when the blends possess a particle-in-matrix morphology. The E' values of the blends in this temperature range decrease nearly linearly with increasing PA content in the blends over the whole composition (as shown in Fig. 16). The minimum, which occurred at room temperature for the noncompatibilized blends on the E'—composition curves (see Fig. 11), disappeared from the curves for the modified blends. These results on the E' curves could be attributed to the fact that the use of PP bearing a functional group reactive to PA resulted in effectively increasing interfacial adhesion between the PP and the PA in the blends and consequently leading to a much finer dispersion morphology when compared with the nonmodified ones. This point can be confirmed by the following SEM micrographs of cryogenically fractured DMA specimens.

The SEM micrographs shown in Figure 17 illustrate that while the compatibilized PP–PA blends do show a two-phase morphology feature throughout the composition range tested, the mixing of the phases has been greatly improved due to compatibilization. It is worth noting that the level of improvement in dispersion for the blends varies with the composition. When the content of the two components are comparable, the blends do not show clear phase separation, and it is difficult to determine the detail of the PP or the PA phases in the blends. For a dispersed phase content of 10% by weight, the blends with PA as dispersed phases have better dispersity than the blends with PP as domains in the PA matrix. This morphological result agrees with the mode of interaction occurring across the PA–PO interface[13] and is supported by the E' data.

The viscosity–composition curves (shown in Fig. 18) provide further evidence of enhanced interactions in the functionized PP–PA-11 blends. The viscosity of the compatibilized blends exhibits a positive deviation from linearity, indicating that a strong interaction occurred during melt blending. The viscosity maximum on the curve exists at around 30% PP content. A negative deviation for the noncompatibilized blends, which is observed on the viscosity–composition curve, should be attributed to the lack of adhesion between two phases.[11] In order to understand the marked effect of the presence of the acid functionality on the PP blends with PA on the properties investigated, two major contributions have to be taken into account as follows: Compatibilization resulting from formation of a graft PP–PA copolymer during the mixing process[6] and the effect of the polar nature of the dispersed phase.[3] Data from the dynamic moduli (E'' and E') curves as well as the morphological and the rheological analyses indeed confirmed the occurrence of those modifications.

The loss factor tan δ (E''/E') spectra are shown in Figures 14 and 19. The results of the tan δ data comparison between the compatibilized and the noncompatibilized blends are more or less surprising. The β-transition peak maxima (T_β) of the PA phase in the carboxyl-functionized PP blends over the whole composition shifted to a higher temperature at about 70°C, which is higher than the T_β at about 60°C for the PA component. In addition, the peaks are broader and tend to drag a shoulder on

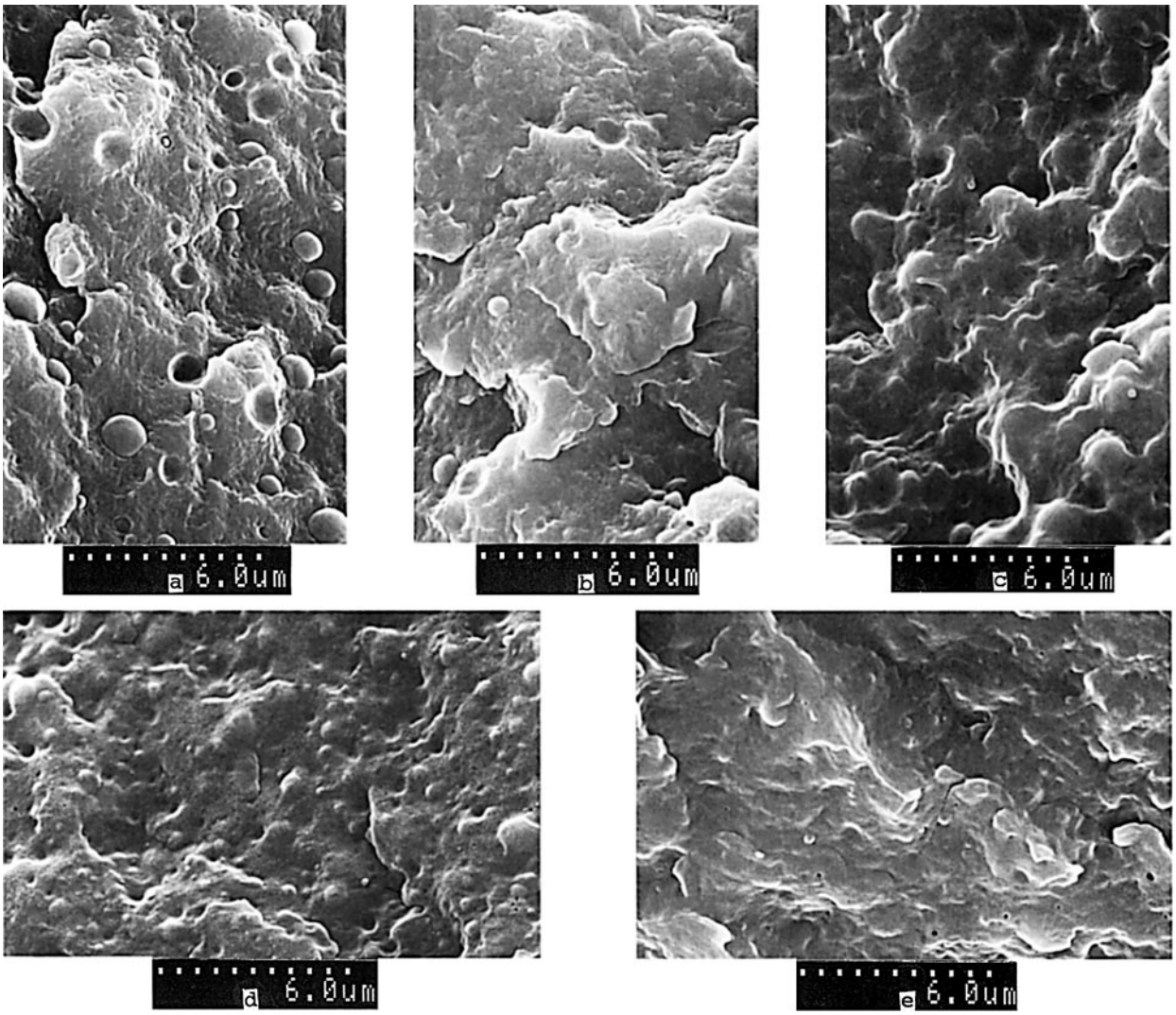

Figure 17 Scanning electron micrograph of fractured surfaces for the compatibilized blends with various PP–PA ratios (a) 1/9, (b) 3/7, (c) 5/5, (d) 7/3, (e) 9/1.

the high-temperature side, especially obvious for the blend at about 50/50 ratio.

However, the result regarding the β-peak shift could not be considered as an indication of a true shift of the glassy transition (T_g) of the PA in the blends because the E'' data for the same blends did not suggest such a shift (see Fig. 13). And also the effect of moisture and orientation on these results presumedly can be ruled out according to the DMA analysis and the morphological observation obtained since all specimens tested were treated identically. Therefore, it may be safe to assume that the distinct β-relaxation feature shown on the tan δ curves for the PA phase would be related to the presence of the acid functionality on the PP in the blends. While both the E'' and the tan δ data in this section suggest that the compatibilization seems to influence the PA phase more than the PP phase in the blends, the testing results for the compatibilized blends indicate that the tan δ spectra appear to show a more complex pattern on the β relaxation of the PA phase than the E'' curves.

According to some authors,[24,25] based on their tan δ data on PA-6, the β relaxation should be a consequence of overlapping of two type transitions: the β (amorphous) relaxation (or T_g) and the crystalline α–γ transition of the PA polymer. Brown and Campbell[25] have used moisture adsorption to separate the β (amorphous) relaxation from this crystalline relaxation, which occurred at about 75°C. Takayanagi[24] found this crystalline relaxation as a shoulder on the high-temperature side of the tan δ

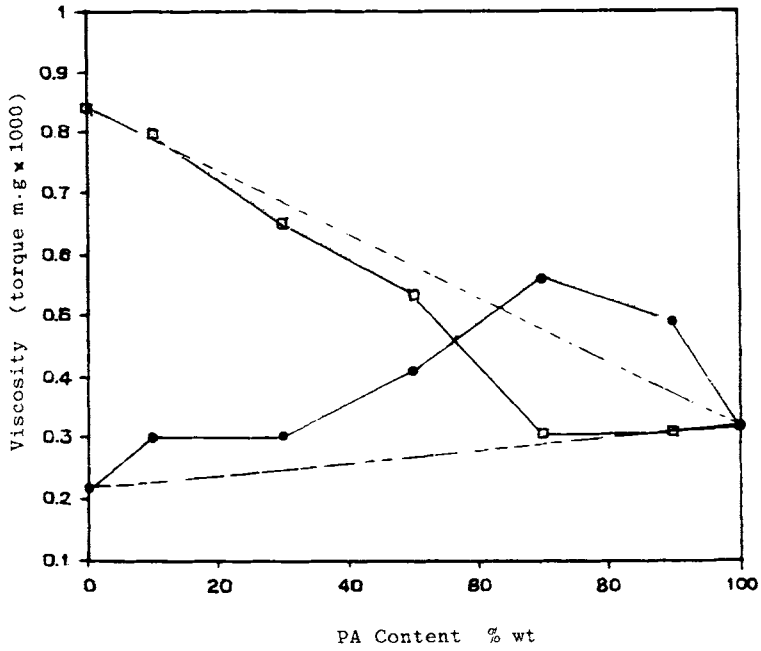

Figure 18 Viscosity (stable torque) of compatibilized blends (●) and noncompatibilized blends (□) as a function of PA content (process condition: 220°C, 100 rpm).

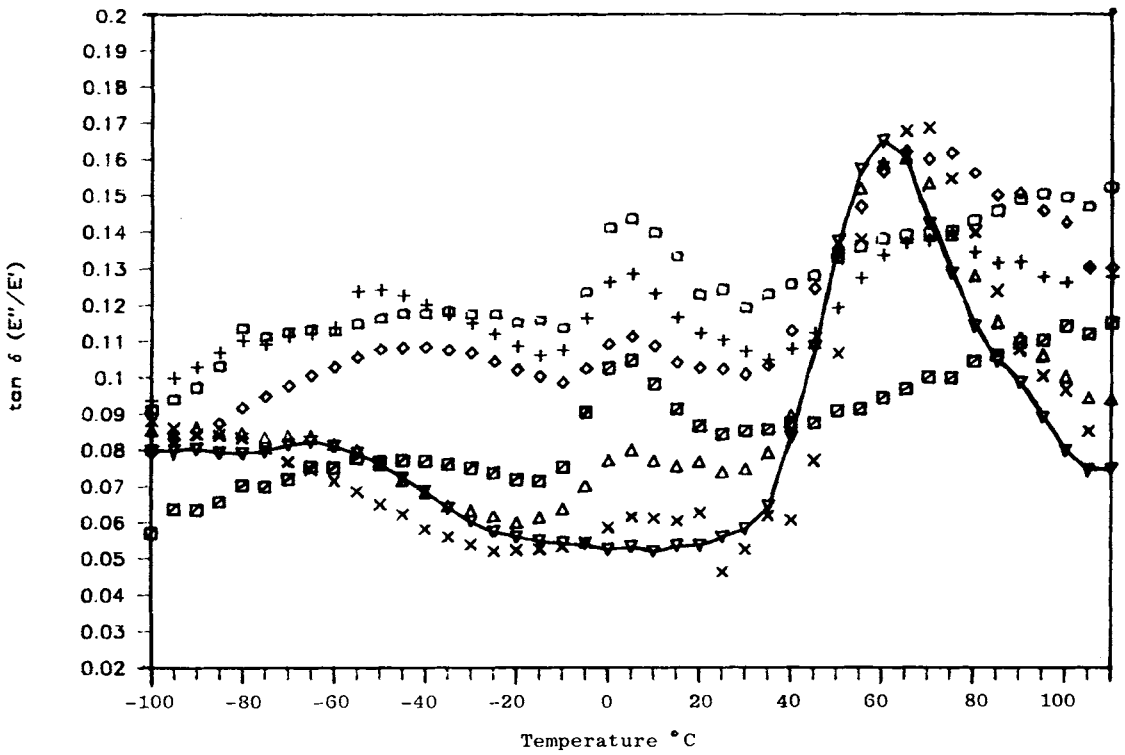

Figure 19 Variation in tan δ with temperature for compatibilized blends at various (PP–PA) ratios (10/0: ▨, 9/1: □, 7/3: +, 5/5: ◇, 3/7: △, 1/9: ×, 0/10: ▽).

peak associated with the β transition and indicated this shoulder was more prominent for the PA specimens with higher crystallinity. For the compatibilized PP–PA-11 blends, the differences in the β peaks of the PA, reflected on the tan δ curves with respect to the nonmodified ones, have some similarity with the broadening and shifting to the higher temperature, described by Takayanagi for the β-transition peaks of the PA-6 with varying crystallinity. Based on this discussion, it is also possible that the functionized PP blends with PA-11 could bring out some influence on PA crystal structure or crystallinity under the specimen preparation condition regulated. Some direct evidence in this aspect will be sought with interest in a further study.

CONCLUSIONS

The compatibilization in the PP–PA-11 binary blends has been achieved through a reactive melt mixing process in a co-rotating twin-screw extruder, followed by compression molding. In the blends an acrylic acid functionized PP was used as a blend component and compared with a nonfunctionized one over the whole concentration range.

The comparative results indicate that the compatibilized blends have finely dispersed morphology and good adhesion between the two phases, especially when the contents of the components are comparable. The viscosity–composition curves exhibit a positive deviation for the compatibilized blends and a negative deviation for the unmodified ones. These effects can be attributed to the reduced interfacial tension as a result of enhanced interactions between the blend components. Dynamic mechanical characterization can provide some further evidence of enhanced interactions.

The testing results show that the storage moduli E' of the compatibilized blends vary nearly linearly as a function of composition in a broad temperature region, while those of the noncompatibilized ones deviate greatly from linearity, specially at about 50/50 ratio, at which a minimum exists at around 20°C. While the dynamic testing gave no evidence of variation in the glassy transition temperatures (peak maxima) of the components (PP and PA) in two types of blends, both the loss modulus (E'') and the loss factor (tan δ) data indicate that the compatibilized blends differ from the noncompatibilized blends mainly in the β-relaxation (or the glassy transition) process of the PA phase, suggesting the compatibilization seems to influence the PA phase more than the PP phase in the blends. But, for the β-relaxation behavior of the PA phase in the modified blends, the tan δ spectra show a more complex pattern than does the E''. While this difference has been discussed in terms of possible chemical/physical influence on the crystalline properties of the PA phase in the blends, its exact nature is uncertain.

The authors thank the Natural Sciences and Engineering Research Council of Canada for the grant that supported this study.

REFERENCES

1. O. Olabisi, L. M. Robeson, and M. T. Shaw, *Polymer–Polymer Miscibility,* Academic Press, New York, 1979, Section 2, Chapter 7.
2. D. R. Paul and S. Newman, Eds., *Polymer Blends,* Vol. I, Academic Press, New York, 1978, Chapter 6, p. 244.
3. M. Xanthos, M. W. Young, and J. A. Beisenberger, *Polym. Eng. Sci.,* **30,** 355 (1990).
4. D. Heikens and W. Barentsen, *Polymer,* **18,** 69 (1979).
5. M. Xanthos, *Polym. Eng. Sci.,* **28,** 1392 (1988).
6. W. J. Macknight, R. W. Lenz, P. V. Masto, and R. J. Somani, *Polym. Eng. Sci.,* **25,** 1124 (1985).
7. P. Galli, S. Danesi, and T. Simonazzi, *Polym. Eng. Sci.,* **24,** 544 (1984).
8. P. Bataille, S. Boisse, and H. P. Schreiber, *Polym. Eng. Sci.,* **27,** 622 (1987).
9. T. Megumi et al., Japanese Patent 63,215,714, A2, (1988).
10. F. Ide and A. Hasegawa, *J. Appl. Polym. Sci.,* **18,** 963 (1974).
11. H. K. Chuang and C. D. Han, in *Polymer Blends and Composites in Multiphase Systems,* C. D. Han, Ed., Am. Chem. Soc., Washington, D.C., 1984, Chapter 11.
12. G. Fairley and R. E. Prud'homme, *Polym. Eng. Sci.,* **28,** 1495 (1987).
13. J. M. Willis and B. D. Favis, *Polym. Eng. Sci.,* **28,** 1416 (1987).
14. C. C. Chen, G. Fontan, K. Min, and J. L. White, *Polym. Eng. Sci.,* **28,** 69 (1988).
15. S. Y. Hobbs, R. C. Bopp, and V. H. Hatkins, *Polym. Eng. Sci.,* **23,** 380 (1983).
16. S. J. Park, B. K. Kim, and H. M. Jeong, *Eur. Polym. J.,* **26,** 131 (1990).
17. M. Takayanagi, K. Imada, A. Nagai, T. Tatsumi, and T. Mastsuo, *J. Polym. Sci., Part C,* **16,** 867 (1967).
18. I. Inamura, H. Ochiai, and H. Yamamura, *J. Polym. Sci. Polym. Phys. Ed.,* **14,** 1221 (1976).
19. N. G. McCrum, B. E. Read, and G. Williams, *Anelastic and Dielectric Effects in Polymeric Solids,* Willy, New York, 1967, pp. 377 and 479.

20. J. Karger-Kocsis and L. Kiss, *Polym. Eng. Sci.*, **27,** 254 (1987).
21. E. Martuscelli, *Polym. Eng. Sci.*, **24,** 563 (1984).
22. E. S. Ong, Y. Kim, and H. L. Williams, *J. Appl. Polym. Sci.*, **31,** 367 (1986).
23. J. P. Bell and T. Murayama, *J. Polym. Sci., A-2,* **7,** 1059 (1969).
24. M. Takayanagi, *Rept. Progr. Polym. Phys. Jpn.*, **6,** 121 (1963).
25. W. B. Brown and G. A. Campbell, paper presented at American Chemical Society Meeting, New York, Sept., 1969; *Polym. Preprints,* **10,** 649 (1969).
26. S. D. Sjoerdsma, J. Dalmolen, A. C. M. Bleijenberg, and D. Heikens, *Polymer,* **21,** 1469 (1980).
27. H. P. Schreiber and M. Kapuscinski, *Polym. Eng. Sci.*, **21,** 433 (1981).
28. C. E. Locke and D. R. Paul, *J. Appl. Polym. Sci.*, **17,** 2597 (1973).
29. F. P. L. Mantia and A. Valenza, *Eur. Polym. J.*, **25,** 553 (1989).
30. L. A. Utracki and P. Sammut, a poster presented at the 33rd IUPAC International Symposium on Macromolecules, Montreal, July, session 1.1.9 (1990).

Received October 25, 1990
Accepted April 8, 1991